

Policy Optimization with Robustness Certificates

Chenxi Yang¹ Greg Anderson¹ Swarat Chaudhuri¹

Abstract

We present a policy optimization framework in which the learned policy comes with a machine-checkable *certificate of adversarial robustness*. Our approach, called CAROL, learns a model of the environment. In each learning iteration, it uses the current version of this model and an external *abstract interpreter* to construct a differentiable signal for provable robustness. This signal is used to guide policy learning, and the abstract interpretation used to construct it directly leads to the robustness certificate returned at convergence. We give a theoretical analysis that bounds the worst-case accumulative reward of CAROL. We also experimentally evaluate CAROL on four MuJoCo environments. On these tasks, which involve continuous state and action spaces, CAROL learns certified policies that have performance comparable to the (non-certified) policies learned using state-of-the-art robust RL methods.

1. Introduction

Reinforcement learning (RL) is an established approach to control tasks (Polydoros & Nalpantidis, 2017; Mnih et al., 2015), including ones in which safety is critical (Cheng et al., 2019a; Sallab et al., 2017). However, state-of-the-art RL methods use deep neural networks as policy representations. This makes them vulnerable to adversarial attacks in which carefully crafted perturbations to a policy’s inputs cause it to behave incorrectly. These problems are even more serious in RL than in supervised learning, as the effects of successive mistakes can cascade over a long time horizon.

These challenges have motivated research on RL algorithms that are robust to adversarial perturbations. In general, methods for adversarial learning can be divided into best-effort heuristic defenses and *certified* approaches that guarantee provable adversarial robustness. The latter are preferable

as heuristic defenses are often defeated by counterattacks (Russo & Proutiere, 2019). In the supervised learning setting, many certified learning techniques have been proposed over the years (Mirman et al., 2018; Cohen et al., 2019; Wong & Kolter, 2018). However, developing such methods for the RL setting has been difficult because of the presence of a blackbox environment. To ensure the robustness of an RL policy, one needs to reason about repeated interactions between the policy, the environment, and the adversary. There is no general approach to doing so. Existing approaches to deep certified RL typically sidestep the challenge through various simplifying assumptions, for example, that the perturbations are stochastic rather than adversarial (Kumar et al., 2021), that the certificate only applies to one-shot interactions between the policy and the environment (Oikarinen et al., 2021; Zhang et al., 2020), or that the action space is discrete (Lütjens et al., 2020).

In this paper, we develop a framework for certifiably robust policy optimization that fills this gap in the literature. We observe that we can reason about adversarial dynamics over entire episodes by learning a *model* of the environment and repeatedly composing it with the policy and the adversary. To this end, we consider a state-adversarial Markov Decision Process (Zhang et al., 2020) in which the observed states are adversarially attacked states of the original environment. During exploration, our algorithm learns a model of the environment using an existing model-based policy optimization algorithm (Janner et al., 2019). We perform *abstract interpretation* (Cousot & Cousot, 1977; Mirman et al., 2018) over compositions of the current policy and the learned environment model to estimate worst-case bounds on the agent’s adversarial reward. The lower bound on the reward is then used to guide policy optimization.

A key benefit of abstract interpretation is that it not only computes bounds on a policy’s worst-case reward but also offers a *proof* of this fact if it holds. A *certificate of robustness* in our framework consists of such a proof.

Our results include a theoretical analysis of our learning algorithm, which shows that our learned certificates give probabilistically sound lower bounds on the accumulative reward of any allowed adversary. We also empirically evaluate CAROL over four high-dimensional MuJoCo environments (Hopper, Walker2d, Halfcheetah, and Ant). We demonstrate

¹UT Austin. Correspondence to: Chenxi Yang <cxyang@cs.utexas.edu>, Greg Anderson <ganderso@cs.utexas.edu>, Swarat Chaudhuri <swarat@cs.utexas.edu>.

that CAROL is able to successfully learn certified policies for these environments and that our strong certification requirements do not compromise empirical performance.

To summarize, our main contributions are as follows:

- We offer CAROL, the first RL framework to guarantee episode-level certifiable adversarial robustness in the presence of continuous states and actions. The framework is based on a new combination of model-based learning and abstract interpretation that can be of independent interest.
- We give a rigorous theoretical analysis that establishes the (probabilistic) soundness of CAROL.
- We give an empirical evaluation that establishes CAROL as a new state of the art for certifiably robust RL.

2. Background

Markov Decision Processes (MDPs). We start with the standard definition of an *Markov Decision Process* (MDP) $\mathcal{M} = (\mathcal{S}, \mathcal{A}, r, P, S_0)$, where \mathcal{S} is a set of states, \mathcal{A} is a set of actions, S_0 is a distribution of initial states, $P(s' | s, a)$ for $s, s' \in \mathcal{S}$ and $a \in \mathcal{A}$ is a probabilistic transition function, and $r(s, a)$ for $s \in \mathcal{S}, a \in \mathcal{A}$ is a real-valued reward function. Our method assumes an additional property that is commonly satisfied in practice: that $P(s' | s, a)$ has the form $\mu_P(s, a) + f_P(s')$, where $f_P(s')$ is a distribution independent of (s, a) and μ_P is deterministic.

A *policy* in \mathcal{M} is a distribution $\pi(a | s)$ with $s \in \mathcal{S}$ and $a \in \mathcal{A}$. A (finite) *trajectory* τ is a sequence $s_0, a_0, s_1, a_1, \dots$ such that $s_0 \sim S_0$, each $a_i \sim \pi(s_i)$, and each $s_{i+1} \sim P(s' | s_i, a_i)$. We denote by $R(\tau) = \sum_i r(s_i, a_i)$ the aggregate (undiscounted) reward along a trajectory τ , and by $R(\pi)$ the expected reward of trajectories unrolled under π .

State-Adversarial MDPs. We model adversarial dynamics using *state-adversarial MDPs* (Zhang et al., 2020). Such a structure is a pair $\mathcal{M}_\nu = (\mathcal{M}, B)$, where $\mathcal{M} = (\mathcal{S}, \mathcal{A}, r, P, S_0)$ is an MDP, and $B : \mathcal{S} \rightarrow 2^{\mathcal{S}}$ is a *perturbation map*.

Suppose we have a policy π in the underlying MDP \mathcal{M} . In an attack scenario, an adversary ν perturbs the *observations* of the agent at a state s . As a result, rather than choosing an action from $\pi(a | s)$, the agent now chooses an action from $\pi(a | \nu(s))$. However, the environment transition is still sampled from $P(s' | s, a)$ and *not* $P(s' | \nu(s), a)$, as the ground-truth state does not change under the attack. We denote by $\pi \circ \nu$ the state-action mapping that results when π is used under this attack scenario.

Naturally, if ν can arbitrarily perturb states, then adversarially robust learning is intractable. Consequently, we constrain ν using B , requiring $\nu(s) \in B(s)$ for all $s \in \mathcal{S}$. We denote the set of allowable adversaries in \mathcal{M}_ν as

$$\mathbb{A}_B = \{\nu : \mathcal{S} \rightarrow \mathcal{S} \mid \forall s \in \mathcal{S}. \nu(s) \in B(s)\}.$$

Abstract Interpretation. We certify adversarial robustness using *abstract interpretation* (Cousot & Cousot, 1977), a classic framework for worst-case safety analysis of systems. Here, one represents sets of system states using symbolic representations (*abstract states*) in a predefined language. For example, we can set our abstract states to be hyperintervals that maintain upper and lower bounds in each dimension of the state space. We denote abstract values with the superscript $\#$, and we use brackets $\llbracket \cdot \rrbracket^\#$ to indicate that we are using abstract semantics. For a set of concrete states S , $\alpha(S)$ denotes the smallest abstract state which contains S . For an abstract state $s^\#$, we denote by $\beta(s^\#)$ the set of concrete states represented by $s^\#$.

The core of abstract interpretation is the propagation of abstract states $s^\#$ through a function $f(s)$ that captures single-step system dynamics. This function can be represented in a variety of ways, including neural networks (Gehr et al., 2018). For propagation, we assume that we have access to a map $f^\#(s^\#)$ that “lifts” f to abstract states. This function must satisfy the property $\beta(f^\#(s^\#)) \supseteq \{f(s) : s \in \beta(s^\#)\}$. Intuitively, $f^\#$ *overapproximates* the behavior of f : while the abstract state $f^\#(s^\#)$ may include some states that are not actually reachable through the application of f to states encoded by $s^\#$, it will *at least* include *every* state that is reachable this way.

By starting with an abstraction $s_0^\#$ of the initial states and using abstract interpretation to propagate this abstract state through the transition function f , we can obtain an abstract state $s_i^\#$ which includes all states of the system that are reachable in i steps, for increasing i . The sequence of abstract states $\tau^\# = s_0^\# s_1^\# s_2^\# \dots$ is called an *abstract trace*.

3. Problem Formulation

To formulate our problem, we first need to define robustness. Assume a fixed adversarial MDP \mathcal{M}_ν , a policy π , and a *robustness threshold* $\Delta > 0$. A *robustness property* is a constraint $\phi(\pi, \Delta)$ of the form

$$\forall \nu \in \mathbb{A}_B. R(\pi) - R(\pi \circ \nu) < \Delta. \quad (1)$$

Intuitively, ϕ requires that no allowable adversary can reduce the expected reward of the policy by more than Δ .

Our goal in this paper is to learn policies that are not just robust but *provably* so. Accordingly, we expect our learning algorithm to produce, in addition to a policy π , a *certificate*, or proof, c of robustness.

Formally, let Π be the universe of all policies in a given state-adversarial MDP $\mathcal{M}_\nu = (\mathcal{M}, B)$. For a policy π and a robustness property ϕ , we write $\pi \vdash_c \phi$ if π *provably* satisfies ϕ , and c is a proof of this fact.

$s_0 = 1$	$\nu(s) = \langle s_0 + \epsilon_0, s_1 + \epsilon_1 \rangle$	s_0	$s_{\text{obs}0}$	a_0	s_1	$s_{\text{obs}1}$	a_1	$R(\pi \circ \nu)$	$\mathbb{E}_{\tau \sim \pi \circ \nu}[R]$
No-Adv	$\epsilon_0 = \epsilon_1 = 0.0$	1	1	1	$2 + e \sim \mathcal{N}(0, 1)$	$2 + e$	$2 + e$	$6 + 2e$	6
Adv-1	$\epsilon_0 = 0.1, \epsilon_1 = -0.4$	1	1.1	1.1	$2.1 + e \sim \mathcal{N}(0, 1)$	$1.7 + e$	$1.7 + e$	$5.9 + 2e$	5.9
Adv-2	$\epsilon_0 = -0.2, \epsilon_1 = -0.3$	1	0.8	0.8	$1.8 + e \sim \mathcal{N}(0, 1)$	$1.5 + e$	$1.5 + e$	$5.1 + 2e$	5.1
Reward Bound ($R^\#$)	$\epsilon_t \in [-0.5, 0.5], \epsilon_t^\# \in [-0.5, 0.5]$	1	$1 + [-0.5, 0.5]$	$[0.5, 1.5]$	$[1.5, 2.5] + e \sim \mathcal{N}(0, 1)$	$[1, 3] + e$	$[1 + e, 3 + e]$	$[4 + 2e, 8 + 2e]$	$[4, 8]$

Table 1: Example of reward bound calculation. The MDP in this example has initial state set $S_0 = \{1\}$, white-box transition function $P(s'|s, a) = s + a + \mathcal{N}(0, 1)$, reward function $r(s, a) = s + a$, and adversary $\nu(s) \in [s - 0.5, s + 0.5]$. ϵ_t denotes the disturbance added on step t . We aim to certify over the worst-case accumulative reward of a deterministic policy π defined as $\pi(s) = s$. We define the *worst-case* here by considering all potential adversaries while still considering the expected behavior over the stochastic environment, P . As shown in the above table, we first demonstrate three traces from fixed adversaries. In the last row, we demonstrate the way how we consider all the adversary behaviors through an abstract trace via abstract interpretation with intervals. The worst-case accumulative reward in this example is 4 as $\mathbb{E}_{\mathcal{N}}[e] = 0$. The abstract trace over all the adversaries in the last row is our certificate which serves as a proof that the policy satisfies our property. We want to ensure the lower bound of the $R^\#$ should not be lower than a threshold. In training, we use the abstract trace to compute a loss to guide the policy optimization process.

The problem of *policy optimization with robustness certificates* is now defined as:

$$\begin{aligned}
 (\pi^*, c) = \arg \max_{\pi \in \Pi} \mathbb{E}_{\tau \sim (\mathcal{M}, \pi)} [R(\tau)] \\
 \text{s.t. } \pi^* \vdash_c \phi.
 \end{aligned} \quad (2)$$

That is, we want to find a policy that maximizes the standard expected reward of the policy, but also ensures that the expected worst-case reward under adversarial dynamics is provably above a threshold.

Our certificates can be constructed using a variety of symbolic or statistical techniques. In CAROL, certificates are constructed using an abstract interpreter. Suppose we have a policy π and an abstract trace $\tau^\# = s_0^\# s_1^\# \dots s_n^\#$ such that for all length- n trajectories $\tau = s_0 \dots s_n$ and all i , $s_i \in \beta(s_i^\#)$. The abstract trace allows us to compute a lower bound on the expected reward for π and also serves as a proof of this bound. We give an example of such certification in a simple state-adversarial MDP, assumed to be available in white-box form, in Table 1.

A challenge here is that abstract interpretation requires a white-box transition function, which is not available in RL. We overcome this challenge by learning a model of the environment during exploration. Model learning is a source of error, so our certificates are probabilistically sound, i.e., they guarantee robustness with high probability. However, this error only depends on the underlying model-based RL algorithm and does not restrict the adversary.

4. Learning Algorithm

Now we present the CAROL framework. The framework (Figure 1) has two key components: a model-based learner and an abstract interpreter. During each training round, the learner maintains a model of the environment dynamics and a policy. These are sent to the abstract interpreter, which calculates a lower bound on the abstract reward. The

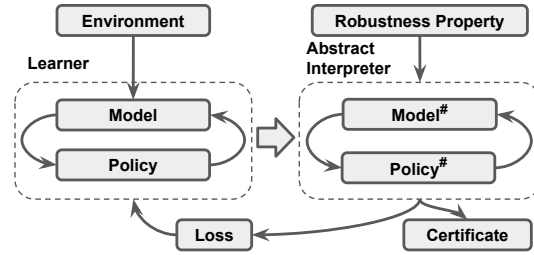


Figure 1: Schematic of CAROL

lower bound is used to compute a differentiable loss that the learner uses in the next iteration of policy optimization. At convergence, the abstract trace computed during abstract interpretation is returned as a certificate of robustness.

Abstract Interpretation in CAROL. Now we describe the abstract interpreter in CAROL in more detail. Recall that our definition of robustness compares the *expected* reward of the original policy to the *expected* reward of the policy under an adversarial perturbation. As a result, our verifier is designed to reason about the worst-case reward under adversarial perturbations, while considering average-case behavior for stochastic policies and environments. Algorithm 1 finds a lower bound on this worst-case expected reward using abstract interpretation to overapproximate the adversary’s possible behaviors along with sampling to approximate the average-case behavior of the policy and environment. We denote this lower bound from Algorithm 1 as *worst-case accumulative reward* (WCAR), which is also used to measure the certified performance in our evaluation.

In more detail, Algorithm 1 proceeds by sampling a starting state $s_0 \sim \mathcal{S}_0$. Then in Algorithm 2 for each time step, we find an overapproximation $s_{\text{obs}_i}^\#$ which includes all of the possible ways the adversary may perturb s_i . Based on this approximation, we *sample* a new approximation from the policy π . Intuitively, this may be done by using a policy π whose randomness does *not* depend on the current state of

Algorithm 1 Worst-Case Accumulative Reward (WCAR)

```

1: Input: policy  $\pi$ , model  $E$ 
2: Output: worst case reward of  $\pi$  under any adversary
3: for  $t$  from 1 to  $N$  do
4:   Sample an initial state  $s_0 \sim \mathcal{S}_0$ 
5:   Get the worst case reward  $R_{\min_t}$  using Algorithm 2 over horizon  $T$  starting from  $s_0$ 
6: end for
7: return  $\frac{1}{N} \sum_{t=1}^N R_{\min_t}$ 
    
```

Algorithm 2 Worst-case rollout under adversarial perturbation

```

1: Input: Initial state  $s_0$ , rollout horizon  $T$ 
2: Output: Worst-case reward of  $\pi$  starting from  $s_0$  over one random trajectory
3: Abstract the initial state and reward:  $s_{\text{original}_0}^\# \leftarrow \alpha(\{s_0\})$ ,  $R_{\min_t}^\# \leftarrow \alpha(\{0\})$ 
4: for  $i$  from 1 to  $T$  do
5:   Abstract over possible perturbations:  $s_{\text{obs}_i}^\# \leftarrow \llbracket B(s_{\text{original}_i}^\#) \rrbracket^\#$ 
6:   Calculate symbolic predicted actions:  $a_i^\# \leftarrow \llbracket \pi(s_{\text{obs}_i}^\#) \rrbracket^\#$ 
7:   Calculate symbolic next-step states and rewards:  $s_{\text{original}_{i+1}}^\#, r_i^\# \leftarrow \llbracket E_\theta(s_{\text{original}_i}^\#, a_i^\#) + \alpha(\{x \mid \|x\| \leq \varepsilon_E\}) \rrbracket^\#$ 
8:   Update worst-case reward:  $R_{\min_t}^\# \leftarrow \llbracket R_{\min_t}^\# + r_i^\# \rrbracket^\#$ 
9: end for
10: return  $\inf \beta(R_{\min_t}^\#)$ 
    
```

the system. More formally, $\pi(a \mid s) = \mu_\pi(s) + f_\pi(a)$ where $f_\pi(a)$ is a distribution with zero mean which is independent of s . Then $a_i^\#$ may be computed as $\llbracket \mu_\pi(s_{\text{obs}_i}^\#) + \alpha(\{e\}) \rrbracket^\#$ where $e \sim f_\pi(a)$. Once the abstract action is computed, we may find the new (abstract) state and reward using the environment model E . The model is assumed to satisfy a PAC-style bound, i.e., there exist δ_E and ε_E such that with probability at least $1 - \delta_E$, $\|E(s, a) - P(s, a)\| \leq \varepsilon_E$. The values of δ_E and ε_E can be measured at model construction.

One way to understand Algorithm 1 is to consider pairs of abstract and concrete trajectories in which the randomness is resolved in the same way. Specifically, if $\pi(a \mid s) = \mu_\pi(s) + f_\pi(a)$ and $E(s' \mid s, a) = \mu(s, a) + f_E(s')$, the initial state s_0 combined with the sequence of values $e_i \sim f_\pi(a)$ and $e'_i \sim f_E(s')$ for $0 \leq i \leq T$ uniquely determine a trajectory. For a given set of values, the reward bound $\inf \beta(R_{\min_t}^\#)$ represents the worst-case reward under any adversary *for a particular resolution of the randomness* in the environment and the policy. The outer loop of Algorithm 1 approximates the expectation over these different random values by sampling. Theorem 1 in Section 5 shows formally that with high probability, Algorithm 1 gives a lower bound on the true adversarial reward.

Learning in CAROL Now we discuss how to learn a policy and environment model which may be proven robust by Algorithm 1. At a high level, Algorithm 3 works by introducing a symbolic loss term L_ψ^{symbolic} which measures the

robustness of the policy. Because robustness is a constrained optimization problem, we use this symbolic loss together with a Lagrange multiplier in an alternating gradient descent scheme to find the optimal robust policy. Formally, for a given environment model E , the inner loop in Algorithm 3 solves the optimization problem

$$\arg \min_{\psi} L^{\text{normal}}(\pi_\psi, \mathcal{D}_{\text{model}}) \quad \text{s.t.} \quad L^{\text{symbolic}}(\pi, E) \leq \Delta$$

via the Lagrangian

$$\arg \min_{\psi} \max_{\lambda \geq 0} L^{\text{normal}}(\pi_\psi, \mathcal{D}_{\text{model}}) + \lambda(L^{\text{symbolic}}(\pi, E) - \Delta).$$

We ensure that solving this problem solves the certifiable robustness problem by enforcing the following conditions: (i) E accurately models the environment and (ii) $L^{\text{symbolic}}(\pi, E)$ measures the “provable robustness” of π . Condition (i) is handled by alternating model updates with policy updates, in the style of Dyna (Sutton, 1990), so we will focus on condition (ii).

The computation of L^{symbolic} uses the same underlying abstract rollouts (Algorithm 2) as the verifier described in Algorithm 1. Once again, this algorithm estimates the reward achieved by a policy under worst-case adversarial perturbations but average-case policy actions and environment transitions. We then define the robustness loss as the difference between the nominal loss R° and the *provable* lower bound on the worst-case loss R_{\min} . Now as long as

Algorithm 3 Policy Optimization for Certifiably Robust Reinforcement Learning

```

1: Initialize a random policy  $\pi_\psi$ , random environment model  $E_\theta$ , and empty model dataset  $\mathcal{D}_{\text{model}}$ .
2: Initialize an environment dataset  $\mathcal{D}_{\text{env}}$  by unrolling trajectories under a random policy.
3: for  $N$  epochs do
4:   Train model  $E_\theta$  on  $\mathcal{D}_{\text{env}}$  via maximum likelihood
5:   Unroll  $M$  trajectories into the model under  $\pi_\psi$ ; add to  $\mathcal{D}_{\text{model}}$ 
6:   Take action in environment according to  $\pi_\psi$ ; add to  $\mathcal{D}_{\text{env}}$ 
7:   for  $G$  gradient updates do
8:     Calculate normal policy loss  $L^{\text{normal}}(\pi_\psi, \mathcal{D}_{\text{model}})$  as in MBPO (Janner et al., 2019)
9:     Sample  $\langle s_t, a_t, s_{t+1}, r_t \rangle$  uniformly from  $\mathcal{D}_{\text{model}}$ 
10:    Rollout  $\pi$  starting from  $s_t$  under  $E_\theta$  for  $T_{\text{train}}$  steps and compute the total reward  $R^o$ 
11:    Compute the worst-case reward  $R_{\min}$  using Algorithm 2 over horizon  $T_{\text{train}}$ .
12:    Compute the robustness loss  $L^{\text{symbolic}}(\pi_\psi, E_\theta) \leftarrow R^o - R_{\min}$ 
13:    Update policy parameters:  $\psi \leftarrow \psi - \alpha \nabla_\psi (L^{\text{normal}}(\pi_\psi, \mathcal{D}_{\text{model}}) + \lambda (L^{\text{symbolic}}(\pi_\psi, E_\theta) - \Delta))$ 
14:    Update Lagrange multiplier:  $\lambda \leftarrow \max(0, \lambda + \alpha' (L^{\text{symbolic}}(\pi_\psi, E_\theta) - \Delta))$ 
15:  end for
16:  Unroll  $n$  trajectories in the true environment under  $\pi_\psi$ ; add to  $\mathcal{D}_{\text{env}}$ 
17: end for
    
```

$L^{\text{symbolic}} < \Delta$, we satisfy the definition of robustness given in Section 3 for that specific trace. Repeating these gradient updates gives an approximation of the average-case behavior which is considered in Algorithm 1.

5. Theoretical Analysis

In this section, we explore some key theoretical properties of CAROL. Proofs are deferred to Appendix B.

Theorem 1. Assume the environment transition distribution is $P(s' | s, a) = \mathcal{N}(\mu_P(s, a), \Sigma_P)$ and the environment model is $E(s' | s, a) = \mathcal{N}(\mu_E(s, a), \Sigma_E)$ with Σ_P, Σ_E diagonal. Further, we assume that the model satisfies a PAC-style guarantee: for any state s , action a , and $\epsilon \in \mathcal{S}$, $|\mu_P(s, a) + \Sigma_P^{1/2}\epsilon - (\mu_E(s, a) + \Sigma_E^{1/2}\epsilon)| \leq \epsilon_E$ with probability at least $1 - \delta_E$. For any policy π , let the result of Algorithm 1 be $\hat{R}^\#$ and let the reward of π under the optimal adversary ν^* be R . Then for any $\delta > 0$ with probability at least $1 - \delta$, we have

$$R \geq \hat{R}^\# - \frac{1}{\sqrt{\delta}} \sqrt{\frac{\text{Var}[R^\#]}{N}} - \left(1 - (1 - \delta_E)^T\right) C.$$

where C is a constant (see Appendix B for details of C).

Theorem 1 shows that our checker is a valid (probabilistic) proof strategy for determining if a policy is robust. That is, if we use Algorithm 1 to measure the reward of a policy under perturbation, the result is a lower bound of the true worst-case reward (minus a constant) with high probability, assuming an accurate environment model. The bound in Theorem 1 gives some interesting insights. First, the bound grows as δ shrinks, so as we consider higher confidence levels, we pay the price of a looser bound. Second, the

bound depends on the variance of the abstract reward and the number of samples in an intuitive way — higher variance makes it harder to measure the true reward, and more samples makes the bound tighter. Third, as δ_E increases, the last term of the bound grows, indicating that a less accurate environment model leads to a looser bound. Finally, the bound grows with T , indicating that over longer time horizons, our reward measurement gets less accurate. This is consistent with the intuition that the environment model may drift away from the true environment over long rollouts.

Theorem 2. Algorithm 3 converges to a policy π which is robust and verifiable by Algorithm 1.

Intuitively, the theorem shows that Algorithm 3 solves the certifiable robustness problem, i.e., it converges to a policy which passes the check by Algorithm 1. The proof is straightforward because Algorithm 3 is a standard primal-dual approach to solve the constrained optimization problem outlined in Equation 2 (Nandwani et al., 2019).

6. Evaluation

We study the following experimental questions:

RQ1: Can CAROL learn policies with nontrivial certified reward bounds?

RQ2: How does CAROL compare with other (non-certified) robust RL methods in terms of certified bounds?

RQ3: How does CAROL compare with other robust RL methods in terms of empirical adversarial performance?

RQ4: How does CAROL’s model-based training approach affect performance?

Environments and Setup. Our experiments consider l_∞ -

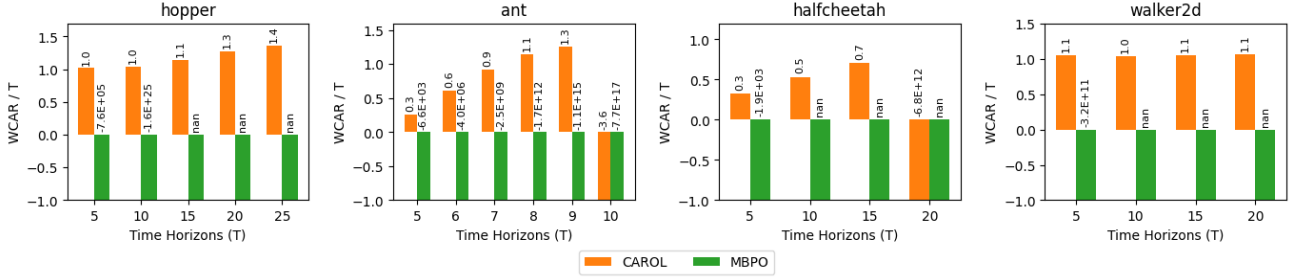


Figure 2: Certified performance of policies π with the learned-together model, E . Each bar is an average of 20 starting states. *nan* denotes *not a number*, which means that (π, E) is not certifiable by a third-party verifier (Zhang et al., 2018). A higher value indicates a better certified *worst-case* performance.

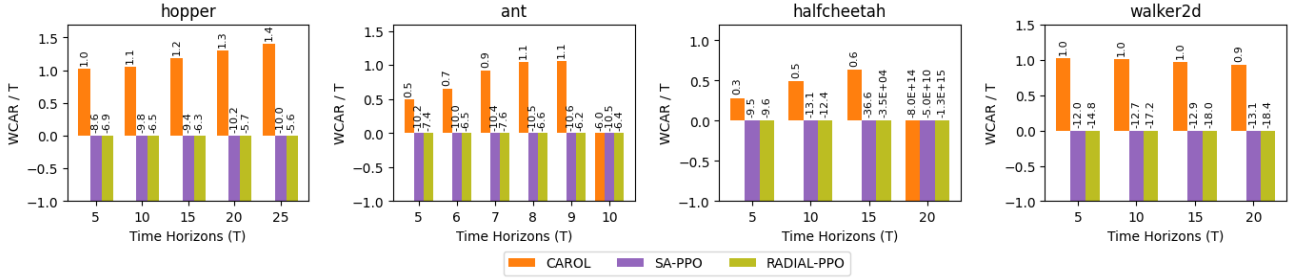


Figure 3: Certified performance of policies π under a set of separately learned models, $\{E_i\}$. Each bar averages the learned policies on each E_i of 20 starting states.

norms perturbation of the state with radius ϵ : $B_p(s, \epsilon) := \{s' \mid \|s' - s\| \leq \epsilon\}$. We implement CAROL on top of the MBPO (Janner et al., 2019) model-based RL algorithm using the implementation from Pineda et al. (2021). For training, we use IBP (Gowal et al., 2018) as a scalable abstract interpretation mechanism. During the evaluation, we use CROWN (Zhang et al., 2018), which is a more expensive but accurate bound propagation method. We use a ϵ -schedule (Gowal et al., 2018; Zhang et al., 2020) during training to slowly increase the ϵ_t at each epoch within the perturbation budget until reaching ϵ . Note that the policies take action stochastically during training, but we set them to be deterministic during evaluation.

We experiment on four MuJoCo environments in OpenAI Gym (Brockman et al., 2016). For CAROL, we use the same hyperparameters as in Pineda et al. (2021) without further tuning. Specifically, we do not use an ensemble of dynamics models. Instead, we use a single dynamic model, which is the case when the ensemble is of size 1. We use Gaussian distribution as the independent noise distribution, $f_\pi(a)$, $f_E(s')$ for both policy and model in the experiments. Concretely, the output of our policies are the parameters μ_π , Σ_π of a Gaussian, with Σ_π being diagonal and independent of input state s . For the model, the output are the parameters μ_E , Σ_E of a Gaussian, with Σ_E being diagonal and independent of input s, a . In the implementation, we approximate the ε_E as zero when measuring the certified

performance for all experiments.

We run Hopper 5×10^5 steps, Walker2d 7.5×10^5 steps, Halfcheetah 8.5×10^5 steps, and Ant 9×10^5 steps for convergence. CAROL has a regularization parameter, λ , for regularizing the robust loss L^{symbolic} , which we set to 1.0, 1.0, 0.5, 0.1 for Hopper, Walker2d, HalfCheetah, and Ant, respectively. We set $T_{\text{train}} = 1$ for all the training of CAROL.

We compare CAROL with the following methods: (1) MBPO (Janner et al., 2019), our base algorithm for policy optimization. (2) SA-PPO (Zhang et al., 2020), a robust RL algorithm bounding per-step action distance. (3) RADIAL-PPO (Oikarinen et al., 2021), a robust RL algorithm using lower bound PPO loss to update the policy. (4) CAROL-Separate Sampler (CAROL-SS), an ablation of CAROL. In CAROL, we update the policy loss L^{normal} with the data sampled from the rollout between the learned model and the policy. While in CAROL-SS, the data for L^{normal} is sampled from the rollout between the environment and the policy. The ϵ_{train} is 0.075, 0.05, 0.075, 0.05 for Hopper, Walker2d, HalfCheetah, and Ant for CAROL, CAROL-SS, SA-PPO, and RADIAL-PPO in this section. More details of the training and setup are available in Appendix C.

Evaluation. We evaluate the performance of policies with two metrics: (i). WCAR following Algorithm 1 for certified performance. (ii). total reward under MAD attacks (Zhang et al., 2020) for empirical performance.

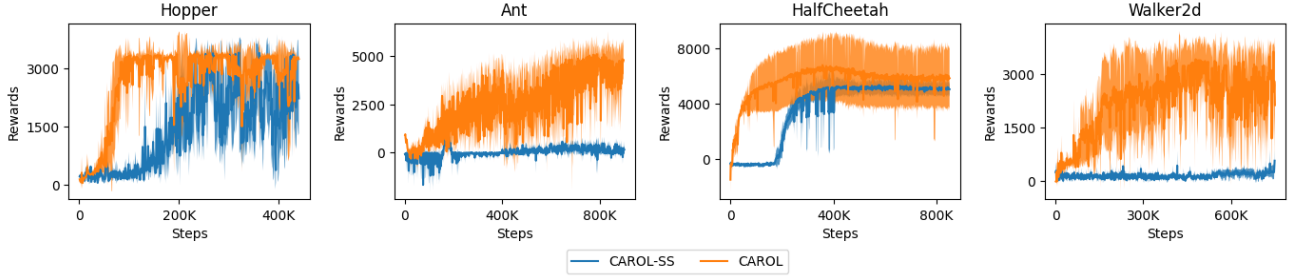


Figure 4: Training Curves of CAROL and CAROL-SS. The solid lines in the graph show the average natural rewards of five training trials, and the shaded areas represent the standard deviation among those trials.

RQ1: Certified Performance with Learned-together Certificate. After training, we get a policy, π , and an environment model, E , trained with the policy. Then, we evaluate the WCAR following Algorithm 1 with π and E . Note that we use an $\epsilon_{\text{test}} = \frac{1}{255}$ for the evaluation of provability as certifying over traces of neural network models accurately is a challenging task for abstract interpreters due to accumulated approximation error. The proof becomes more challenging as the horizon increases as the impact from each step’s worst-case adversary accumulates. We vary the certified horizon under the ϵ_{test} to exhibit the certified performance. To have a fair comparison across different horizons, we quantify the certified performance by WCAR/T .

Figure 2 exhibits the certified performance of CAROL. Both CAROL and MBPO are evaluated with the model trained together. We are able to train a policy with better certified accumulative reward under the worst attacks compared to the base algorithm, MBPO, which does not use the regularization L^{symbolic} . As the time horizon increases, it becomes harder to certify the accumulative reward. For example, in Ant and HalfCheetah, CAROL is not able to give a good certified performance when the horizon reaches 10 and 20 respectively because of the accumulative influence from the worst-case attack and the overapproximation from the abstract interpreter. We also highlight that Ant is a challenging task for certification due to the high-dimensional state space.

RQ2: Comparison of Certified Performance with Other Methods. We compare CAROL with two robust RL methods, SA-PPO (Zhang et al., 2020) and RADIAL-PPO (Oikarinen et al., 2021), which both bound the per-step performance of the policy during training. SA-PPO bounds the per-step action deviation under perturbation, and RADIAL-PPO bounds the one-step loss under perturbation. To have a fair comparison of the certified performance of policies and avoid model error bias, we separately train 5 additional environment models, $\{E_i\}$, with the trajectory datasets unrolled from 5 additional policies (with regular RL training) and the environment. We truncate CAROL by extracting the policies from training and certify them with these separately

Environment	Model	Nominal $\epsilon = 0$	Attack (MAD) $\epsilon = \epsilon_{\text{train}}$
Hopper ($\epsilon_{\text{train}} = 0.075$)	MBPO	3246.0 \pm 76.1	2874.2 \pm 203.4
	SA-PPO	3423.9 \pm 164.2	3213.8\pm284.8
	RADIAL-PPO	3547.0\pm166.9	3100.3 \pm 368.3
	CAROL	3290.1 \pm 104.9	3201.4 \pm 100.5
Ant ($\epsilon_{\text{train}} = 0.05$)	MBPO	4051.9 \pm 526.2	406.2 \pm 83.5
	SA-PPO	5368.8 \pm 96.4	5327.4 \pm 112.7
	RADIAL-PPO	4694.1 \pm 219.5	4478.9 \pm 232.8
	CAROL	5696.6\pm277.9	5362.2\pm242.8
HalfCheetah ($\epsilon_{\text{train}} = 0.075$)	MBPO	7706.3\pm710.1	2314.6 \pm 566.7
	SA-PPO	3193.9 \pm 650.7	3231.6 \pm 659.9
	RADIAL-PPO	3686.5 \pm 439.2	3409.6 \pm 683.9
	CAROL	5821.5 \pm 2401.9	3961.6\pm899.5
Walker2d ($\epsilon_{\text{train}} = 0.05$)	MBPO	3815.6 \pm 211.9	3616.5 \pm 228.2
	SA-PPO	4271.7\pm222.2	4444.4\pm286.0
	RADIAL-PPO	2935.1 \pm 272.1	3022.6 \pm 381.7
	CAROL	3784.4 \pm 329.1	3774.3 \pm 260.3

Table 2: Average episodic reward \pm standard deviation over 100 episodes on three baselines and CAROL. We show natural rewards (under no attack) and rewards under adversarial attacks. The best results over all methods are in bold.

trained environment models. This setting is not completely inline with CAROL’s learned certificate and verification (see RQ1) but is designed for a fair comparison across policies.

As shown in Figure 3, the CAROL’s certified performance with separately trained models is slightly worse yet comparable to its performance when using learned-together certificates. When compared with non-certified RL policies, CAROL consistently exhibits better certifiable performance. It is worth noting that CAROL is able to provide increasing worst-case rewards over time for the Hopper, Ant, and HalfCheetah, which aligns with the reward mechanisms used in these environments. Thus, we believe these results demonstrate that CAROL is able to give a reasonable certified performance, while the other methods, which are not specifically designed for worst-case accumulative reward certification, struggle to achieve the same goal.

RQ3: Comparison of Empirical Performance with

Other Methods. Usually, there is a trade-off between certified robustness and empirical robustness. One can get good provability but may sacrifice empirical rewards. We show that policy from our algorithm shows comparable natural rewards (without attack) and adversarial rewards compared with other methods. In Table 2, we show results on 4 environments and comparison with MBPO, SA-PPO, and RADIAL-PPO. The policies are the same ones evaluated for RQ1 and RQ2. For each environment, we compare the performance under MAD attacks (Zhang et al., 2020). CAROL outperforms other methods on Ant and HalfCheetah under attack when the base algorithm, MBPO, is extremely not robust. For Hopper, CAROL has comparable adversarial rewards with the best methods. CAROL’s reward is worse on Walker2d though still reasonable.

RQ4: Impact of Model-Based Training. In this part, we investigate the impact of our design choices for L^{normal} on performance. We compare our framework, CAROL, with an ablation of it, CAROL-SS, to understand how rollout with the learned model for L^{normal} matters in CAROL. We present a comparison of performance during training, as shown in Figure 4. In the implementation, we set a smoother ϵ -schedule for CAROL-SS by allowing CAROL-SS to take longer steps from $\epsilon = 0$ to the target ϵ . These results show that CAROL converges much faster while achieving a comparable or better final performance due to the benefits of the sample efficiency of MBRL. Additionally, the consistency between the rollout datasets for L^{normal} and the ones for L^{symbolic} also leads to a better natural reward at convergence in training.

7. Related Work

Adversarial RL. Adversarial attacks on RL systems have been extensively studied. Specific attacks that have been investigated include adversarial perturbations on agents’ observations or actions (Huang et al., 2017; Lin et al., 2017; Weng et al., 2019), adversarial disturbance forces to the system (Pinto et al., 2017), and other adversarial policies in a multiagent setting (Gleave et al., 2019). Most recently, Zhang et al. (2021) and Sun et al. (2021) propose methods to train agents together with a learned optimal adversary in an online way to achieve better adversarial reward. These efforts are orthogonal to existing regularization-based techniques (including ours).

Robust RL and Provable Robustness in RL. Multiple robust training methods have been applied to deep RL. Fischer et al. (2019) leverage additional student networks to help the robust Q learning, and Everett et al. (2021) enhance an agent’s robustness during testing time by computing the lower bound of each action’s Q value at each step. Zhang et al. (2020) and Oikarinen et al. (2021) leverage a bound propagation technique in a loss regularizer to encourage the agent to either follow its original actions or optimize over a

loss lower bound. While these efforts achieve robustness by deterministic certification techniques for neural networks (Gowal et al., 2018; Xu et al., 2020), they mainly focus on the step-wise certification and are not able to give robustness certification if the impact from attacks accumulates across multiple steps. CAROL differs from these papers by offering certified robustness for the aggregate reward in an episode. We know of only two recent efforts that study robustness certification for cumulative rewards (Wu et al., 2021; Kumar et al., 2021). Of these, (Wu et al., 2021) is a framework for certification rather than certified learning. (Kumar et al., 2021) proposes a certified learning algorithm under the assumption that the adversarial perturbation is smoothed using random noise. The attack model here is weaker than the adversarial model assumed by CAROL and most other work on adversarial learning.

Certified RL. Safe control with learned certificates is an active field (Dawson et al., 2022). A few efforts in this space have considered controllers discovered through RL. Many works use a given certificate with strong control-theoretic priors to constrain the actions of an RL agent (Cheng et al., 2019a; Li & Belta, 2019; Cheng et al., 2019b) or assume the full knowledge of the environment to yield the certificate during the training of an agent (Yang & Chaudhuri, 2021). Chow et al. (2019) and Chow et al. (2018) attempt to derive certificates from the structure of the constrained Markov decision process (Altman, 1999) for the safe control problems. Chang & Gao (2021) incorporate Lyapunov methods in deep RL to learn a neural Lyapunov critic function to improve the stability of an RL agent. We differ from this work by focusing on adversarial robustness rather than stability.

8. Conclusion and Future Work

We have presented CAROL, the first RL framework with certifiable episode-level robustness guarantees. Our approach is based on a new combination of model-based RL and abstract interpretation. We have given a theoretical analysis to justify the approach and also validated it empirically in four challenging continuous control tasks.

A key challenge in CAROL is that our abstract interpreter may not be sufficiently precise, and attempts to increase precision may compromise scalability. Future research should work to address this issue with more accurate and scalable verification techniques. Also, as seen in Figure 4, there is variance in the results due to the use of a single dynamics model. To address this issue, future work should explore ways to incorporate certificates across ensembles of models. Finally, because abstract interpretation of probabilistic systems is difficult, our approach assumes that the randomness in the environment transitions is state-independent. Future work should try to eliminate this assumption through abstract interpreters tailored to probabilistic systems.

References

- Altman, E. *Constrained Markov decision processes: stochastic modeling*. Routledge, 1999.
- Brockman, G., Cheung, V., Pettersson, L., Schneider, J., Schulman, J., Tang, J., and Zaremba, W. Openai gym, 2016.
- Chang, Y.-C. and Gao, S. Stabilizing neural control using self-learned almost lyapunov critics. In *2021 IEEE International Conference on Robotics and Automation (ICRA)*, pp. 1803–1809. IEEE, 2021.
- Cheng, R., Orosz, G., Murray, R. M., and Burdick, J. W. End-to-end safe reinforcement learning through barrier functions for safety-critical continuous control tasks. In *Proceedings of the AAAI Conference on Artificial Intelligence*, volume 33, pp. 3387–3395, 2019a.
- Cheng, R., Verma, A., Orosz, G., Chaudhuri, S., Yue, Y., and Burdick, J. Control regularization for reduced variance reinforcement learning. In *International Conference on Machine Learning*, pp. 1141–1150. PMLR, 2019b.
- Chow, Y., Nachum, O., Duenez-Guzman, E., and Ghavamzadeh, M. A lyapunov-based approach to safe reinforcement learning. *Advances in neural information processing systems*, 31, 2018.
- Chow, Y., Nachum, O., Faust, A., Duenez-Guzman, E., and Ghavamzadeh, M. Lyapunov-based safe policy optimization for continuous control. *arXiv preprint arXiv:1901.10031*, 2019.
- Cohen, J., Rosenfeld, E., and Kolter, Z. Certified adversarial robustness via randomized smoothing. In *International Conference on Machine Learning*, pp. 1310–1320. PMLR, 2019.
- Cousot, P. and Cousot, R. Abstract interpretation: a unified lattice model for static analysis of programs by construction or approximation of fixpoints. In *Conference Record of the Fourth Annual ACM SIGPLAN-SIGACT Symposium on Principles of Programming Languages*, pp. 238–252, Los Angeles, California, 1977. ACM Press, New York, NY.
- Dawson, C., Gao, S., and Fan, C. Safe control with learned certificates: A survey of neural lyapunov, barrier, and contraction methods. *arXiv preprint arXiv:2202.11762*, 2022.
- Everett, M., Lütjens, B., and How, J. P. Certifiable robustness to adversarial state uncertainty in deep reinforcement learning. *IEEE Transactions on Neural Networks and Learning Systems*, 2021.
- Fischer, M., Mirman, M., Stalder, S., and Vechev, M. Online robustness training for deep reinforcement learning. *arXiv preprint arXiv:1911.00887*, 2019.
- Gehr, T., Mirman, M., Drachler-Cohen, D., Tsankov, P., Chaudhuri, S., and Vechev, M. Ai2: Safety and robustness certification of neural networks with abstract interpretation. In *2018 IEEE symposium on security and privacy (SP)*, pp. 3–18. IEEE, 2018.
- Gleave, A., Dennis, M., Wild, C., Kant, N., Levine, S., and Russell, S. Adversarial policies: Attacking deep reinforcement learning. *arXiv preprint arXiv:1905.10615*, 2019.
- Gowal, S., Dvijotham, K., Stanforth, R., Bunel, R., Qin, C., Uesato, J., Arandjelovic, R., Mann, T., and Kohli, P. On the effectiveness of interval bound propagation for training verifiably robust models. *arXiv preprint arXiv:1810.12715*, 2018.
- Haarnoja, T., Zhou, A., Abbeel, P., and Levine, S. Soft actor-critic: Off-policy maximum entropy deep reinforcement learning with a stochastic actor. In *International conference on machine learning*, pp. 1861–1870. PMLR, 2018.
- Huang, S., Papernot, N., Goodfellow, I., Duan, Y., and Abbeel, P. Adversarial attacks on neural network policies. *arXiv preprint arXiv:1702.02284*, 2017.
- Janner, M., Fu, J., Zhang, M., and Levine, S. When to trust your model: Model-based policy optimization. *Advances in Neural Information Processing Systems*, 32, 2019.
- Kumar, A., Levine, A., and Feizi, S. Policy smoothing for provably robust reinforcement learning. In *International Conference on Learning Representations*, 2021.
- Li, X. and Belta, C. Temporal logic guided safe reinforcement learning using control barrier functions. *arXiv preprint arXiv:1903.09885*, 2019.
- Lin, Y.-C., Hong, Z.-W., Liao, Y.-H., Shih, M.-L., Liu, M.-Y., and Sun, M. Tactics of adversarial attack on deep reinforcement learning agents. *arXiv preprint arXiv:1703.06748*, 2017.
- Lütjens, B., Everett, M., and How, J. P. Certified adversarial robustness for deep reinforcement learning. In *Conference on Robot Learning*, pp. 1328–1337. PMLR, 2020.
- Mirman, M., Gehr, T., and Vechev, M. Differentiable abstract interpretation for provably robust neural networks. In *International Conference on Machine Learning*, pp. 3578–3586. PMLR, 2018.

- Mnih, V., Kavukcuoglu, K., Silver, D., Rusu, A. A., Veness, J., Bellemare, M. G., Graves, A., Riedmiller, M., Fidjeland, A. K., Ostrovski, G., et al. Human-level control through deep reinforcement learning. *nature*, 518(7540): 529–533, 2015.
- Nandwani, Y., Pathak, A., Mausam, and Singla, P. A primal dual formulation for deep learning with constraints. In Wallach, H., Larochelle, H., Beygelzimer, A., d’Alché-Buc, F., Fox, E., and Garnett, R. (eds.), *Advances in Neural Information Processing Systems*, volume 32. Curran Associates, Inc., 2019. URL <https://proceedings.neurips.cc/paper/2019/file/cf708fcd1decf0337aded484f8f4519ae-Paper.pdf>.
- Oikarinen, T., Zhang, W., Megretski, A., Daniel, L., and Weng, T.-W. Robust deep reinforcement learning through adversarial loss. *Advances in Neural Information Processing Systems*, 34:26156–26167, 2021.
- Pineda, L., Amos, B., Zhang, A., Lambert, N. O., and Calandra, R. Mbrl-lib: A modular library for model-based reinforcement learning. *Arxiv*, 2021. URL <https://arxiv.org/abs/2104.10159>.
- Pinto, L., Davidson, J., Sukthankar, R., and Gupta, A. Robust adversarial reinforcement learning. In *International Conference on Machine Learning*, pp. 2817–2826. PMLR, 2017.
- Polydoros, A. S. and Nalpantidis, L. Survey of model-based reinforcement learning: Applications on robotics. *Journal of Intelligent & Robotic Systems*, 86(2):153–173, 2017.
- Russo, A. and Proutiere, A. Optimal attacks on reinforcement learning policies. *arXiv preprint arXiv:1907.13548*, 2019.
- Sallab, A. E., Abdou, M., Perot, E., and Yogamani, S. Deep reinforcement learning framework for autonomous driving. *Electronic Imaging*, 2017(19):70–76, 2017.
- Sun, Y., Zheng, R., Liang, Y., and Huang, F. Who is the strongest enemy? towards optimal and efficient evasion attacks in deep rl. *arXiv preprint arXiv:2106.05087*, 2021.
- Sutton, R. S. Integrated architecture for learning, planning, and reacting based on approximating dynamic programming. In *Proceedings of the Seventh International Conference (1990) on Machine Learning*, pp. 216–224, San Francisco, CA, USA, 1990. Morgan Kaufmann Publishers Inc. ISBN 1558601414.
- Weng, T.-W., Dvijotham, K. D., Uesato, J., Xiao, K., Goyal, S., Stanforth, R., and Kohli, P. Toward evaluating robustness of deep reinforcement learning with continuous control. In *International Conference on Learning Representations*, 2019.
- Wong, E. and Kolter, Z. Provable defenses against adversarial examples via the convex outer adversarial polytope. In *International Conference on Machine Learning*, pp. 5286–5295. PMLR, 2018.
- Wu, F., Li, L., Huang, Z., Vorobeychik, Y., Zhao, D., and Li, B. Crop: Certifying robust policies for reinforcement learning through functional smoothing. In *International Conference on Learning Representations*, 2021.
- Xu, K., Shi, Z., Zhang, H., Huang, M., Chang, K., Kailkhura, B., Lin, X., and Hsieh, C. Automatic perturbation analysis on general computational graphs. Technical report, Lawrence Livermore National Lab.(LLNL), Livermore, CA (United States), 2020.
- Yang, C. and Chaudhuri, S. Safe neurosymbolic learning with differentiable symbolic execution. In *International Conference on Learning Representations*, 2021.
- Zhang, H., Weng, T.-W., Chen, P.-Y., Hsieh, C.-J., and Daniel, L. Efficient neural network robustness certification with general activation functions. *Advances in neural information processing systems*, 31, 2018.
- Zhang, H., Chen, H., Xiao, C., Li, B., Liu, M., Boning, D., and Hsieh, C.-J. Robust deep reinforcement learning against adversarial perturbations on state observations. *Advances in Neural Information Processing Systems*, 33: 21024–21037, 2020.
- Zhang, H., Chen, H., Boning, D., and Hsieh, C.-J. Robust reinforcement learning on state observations with learned optimal adversary. *arXiv preprint arXiv:2101.08452*, 2021.

A. Symbols

We give a summary of the symbols used in this paper below.

Definition	Symbol/Notation
Policy	π_{ψ}, π
Model of the environment	E_{θ}, E
Environment transition	P
Parameters (mean, covariance) for Gaussian distribution for environment, model, and policy	$\mu_P, \Sigma_P, \mu_E, \Sigma_E, \mu_{\pi}, \Sigma_{\pi}$
Distribution representing noise for environment, model, and policy	f_P, f_E, f_{π}
Adversary	ν
Regular policy loss	L^{normal}
Robustness loss	L^{symbolic}
Lipschitz constants for the environment model and policy mean	L_E, L_P
Model error	ε_E
PAC bound probability	δ_E
Abstract values and semantics	$\cdot^{\#}, \llbracket \cdot \rrbracket^{\#}$
Abstraction	α
Concretization	β
Horizon for training and testing	$T, T_{\text{train}}, T_{\text{test}}$
Disturbance for training and testing	$\epsilon, \epsilon_{\text{train}}, \epsilon_{\text{test}}$

B. Proofs

In this section we present proofs of the theorems from Section 5.

Assumption 3. The horizon of the MDP is bounded by T .

Assumption 4. The environment transition distribution has the form $P(s' | s, a) = \mathcal{N}(\mu_P(s, a), \Sigma_P)$ with Σ_P diagonal and the environment model E has the form $E(s' | s, a) = \mathcal{N}(\mu_E(s, a), \Sigma_E)$ with Σ_E diagonal.

Assumption 5. There exist values ε_E and δ_E such that for all s, a and for any fixed e with probability at least $1 - \delta_E$, $\left\| \left(\mu_P(s, a) + \Sigma_P^{1/2} e \right) - \left(\mu_E(s, a) + \Sigma_E^{1/2} e \right) \right\| \leq \varepsilon_E$. Further, there exists some d_E such that for all s, a , $\left\| \left(\mu_P(s, a) + \Sigma_P^{1/2} e \right) - \left(\mu_E(s, a) + \Sigma_E^{1/2} e \right) \right\| \leq d_E$.

Assumption 6. The environment model mean function $\mu_E(s, a)$ is L_E -Lipschitz continuous, the immediate reward function $r(s, a)$ is L_r -Lipschitz continuous, and the policy mean $\mu_{\pi}(s)$ is L_{π} -Lipschitz continuous.

Assumption 7. For all $s \in \mathcal{S}$, we have $s \in B(s)$. That is, the adversary may choose not to perturb any state.

Theorem 1. For any policy π , let the result of Algorithm 1 be $\hat{R}^{\#}$, let ν^* be the optimal adversary (i.e., for all $\nu \in \mathbb{A}_B$, $R(\pi \circ \nu^*) \leq R(\pi \circ \nu)$), and let the reward of $\pi \circ \nu^*$ be R . Then for any $\delta > 0$ with probability at least $1 - \delta$, we have

$$\mathbb{E}[R(\tau)] \geq \hat{R}^{\#}(\tau) - \frac{1}{\sqrt{\delta}} \sqrt{\frac{\text{Var}[R^{\#}(\tau)]}{N}} - \left(1 - (1 - \delta_E)^T\right) L_r(1 + L_{\pi}) d_E \frac{(L_E L_{\pi})^T + (1 - L_E L_{\pi})T - 1}{(1 - L_E L_{\pi})^2}.$$

Proof. Recall that the environment transition P and policy π are assumed to be separable, i.e., $P(s' | s, a) = \mu_P(s, a) + f_P(s')$ and $\pi(a | s) = \mu_{\pi}(s) + f_{\pi}(a)$ with μ_P and μ_{π} deterministic. As a result, a trajectory under policy $\pi \circ \nu^*$ may be written $\tau = s_0, a_0, s_1, a_1, \dots, s_n, a_n$ where $s_0 \sim \mathcal{S}_0$, each $a_i = \mu_{\pi}(\nu^*(s_i)) + e_i^{\pi}$ for $e_i^{\pi} \sim f_{\pi}(a)$, and each $s_i = \mu_P(s_{i-1}, a_{i-1}) + e_i^P$ for $e_i^P \sim f_P(s')$. By Assumption 4, we know that $e_i^P \sim \mathcal{N}(\mathbf{0}, \Sigma_P)$ so that $e_i^P = \Sigma_P^{1/2} e_i$ where $e_i \sim \mathcal{N}(\mathbf{0}, \mathbf{I})$. In particular, because each trajectory τ is uniquely determined by $s_0, \{e_i^{\pi}\}_{i=0}^n, \{e_i\}_{i=1}^n$, we can write the reward of $\pi \circ \nu^*$ as

$$R(\pi \circ \nu^*) = \mathbb{E}_{s_0 \sim \mathcal{S}_0, \{e_i^{\pi} \sim f_{\pi}(a)\}_{i=0}^n, \{e_i \sim \mathcal{N}(\mathbf{0}, \mathbf{I})\}_{i=1}^n} R(\tau)$$

Because this expectation ranges over the values of $s_0, \{e_i^{\pi}\}_{i=0}^n, \{e_i\}_{i=1}^n$, we will proceed by considering pairs of abstract and concrete trajectories unrolled with the same starting state and noise terms.

To do this, we analyze Algorithm 2 for some fixed $s_0, \{e_i^\pi\}_{i=0}^n, \{e_i\}_{i=1}^n$. Let $e_i^E = \Sigma_E^{1/2} e_i$. That is, given the same underlying sample from $\mathcal{N}(0, I)$, e_i^P is the noise in the true environment while e_i^E is the noise in the modeled environment. We show by induction that for all i , $s_i \in \beta(s_{\text{original}_i}^\#)$ with probability at least $(1 - \delta_E)^i$. Note that, because abstract interpretation is sound, $s_0 \in \beta(s_{\text{original}_0}^\#)$. Additionally, for all i if $s_i \in \beta(s_{\text{original}_i}^\#)$ then $\nu^*(s_i) \in \beta(s_{\text{obs}_i}^\#)$. Moreover, since e_i^π is fixed, we have

$$\llbracket \pi(s_{\text{obs}_i}^\#) \rrbracket^\# = \llbracket \mu_\pi(s_{\text{obs}_i}^\#) + e_i^\pi \rrbracket^\#$$

so that $\pi(\nu^*(s)) \in \beta(a_i^\#)$. Similarly, because e_i^E is fixed, let $\Delta_E = \alpha(\{x \mid \|x\| \leq \varepsilon_E\})$ and we have

$$\llbracket E(s_{\text{original}_i}^\#, a_i^\#) + \Delta_E \rrbracket^\# = \llbracket \mu_E(s_{\text{original}_i}^\#, a_i^\#) + e_i^E + \Delta_E \rrbracket^\#.$$

By the induction hypothesis, we know that $s_{i-1} \in \beta(s_{\text{original}_{i-1}}^\#)$ with probability at least $(1 - \delta_E)^{i-1}$ and therefore $a_{i-1} \in \beta(a_{i-1}^\#)$. By Assumption 5, we have that $\|(\mu_P(s, a) + e_i^P) - (\mu_E(s, a) + e_i^E)\| < \varepsilon_E$ with probability at least $1 - \delta_E$. In particular, $(\mu_P(s, a) + \varepsilon_i^P) - (\mu_E(s, a) + \varepsilon_i^E) \in \Delta_E$, so that $\mu_P(s, a) + e_i^P \in \beta(\llbracket E(s_{\text{original}_i}^\#, a_i^\#) + \Delta_E \rrbracket^\#)$. Then with probability at least $1 - \delta_E$, if $s_{i-1} \in \beta(s_{\text{original}_{i-1}}^\#)$ then $s_i \in \beta(s_{\text{original}_i}^\#)$. As a result, $s_i \in \beta(s_{\text{original}_i}^\#)$ with probability at least $(1 - \delta_E)^i$. In particular, by Assumption 3, $n \leq T$ so that for a fixed τ defined by $s_0, \{e_i^\pi\}_{i=0}^n, \{e_i\}_{i=1}^n$, we have that with probability at least $(1 - \delta_E)^T$, Algorithm 2 returns a lower bound on $R(\tau)$.

Now we consider the case where Algorithm 2 does *not* return a lower bound of $R(\tau)$. In this case, we show (again by induction) that for all $0 \leq i \leq T$, there exists a point $s'_i \in \beta(s_{\text{original}_i}^\#)$ such that

$$\|s_i - s'_i\| \leq \sum_{j=0}^{i-1} (L_E L_\pi)^j d_E = d_E \left(\frac{1 - (L_E L_\pi)^{i-1}}{1 - L_E L_\pi} \right)$$

(when $\sum_{j=0}^{-1} (L_E L_\pi)^j d_E$ is taken to be zero). First, note that $s_0 \in \beta(s_{\text{original}_0}^\#)$, so the base case is trivially true. Now by the induction hypothesis we have that there exists some $s'_{i-1} \in \beta(s_{\text{original}_{i-1}}^\#)$ with $\|s_{i-1} - s'_{i-1}\| \leq \sum_{j=0}^{i-2} (L_E L_\pi)^j d_E$. Notice that by Assumption 7, we also have $s'_{i-1} \in \beta(s_{\text{obs}_{i-1}}^\#)$. Now because abstract interpretation is sound, we have that $\mu_\pi(s'_{i-1}) + e_{i-1}^\pi \in \beta(a_{i-1}^\#)$ and by Assumption 6, $\|\mu_\pi(s_{i-1}) - \mu_\pi(s'_{i-1})\| \leq L_\pi \sum_{j=0}^{i-2} (L_E L_\pi)^j d_E$. Similarly, we have $\mu_E(s'_{i-1}, \mu_\pi(s'_{i-1}) + e_{i-1}^\pi) + e_{i-1}^E \in \beta(s_{\text{original}_i}^\#)$, and $\|\mu_E(s_{i-1}, \mu_\pi(s_{i-1}) + e_{i-1}^\pi) - \mu_E(s'_{i-1}, \mu_\pi(s'_{i-1}) + e_{i-1}^\pi)\| \leq L_E L_\pi \sum_{j=0}^{i-2} (L_E L_\pi)^j d_E$. Let $\hat{s}_i = \mu_E(s_{i-1}, \mu_\pi(s_{i-1}) + \varepsilon_{i-1}^\pi) + \varepsilon_i^E$. Then by Assumption 5, we have $\|\hat{s}_i - s_i\| \leq d_E$, so that in particular $\|s_i - \mu_E(s'_{i-1}, \mu_\pi(s'_{i-1}) + e_{i-1}^\pi) + \varepsilon_i^E\| \leq d_E + L_E L_\pi \sum_{j=0}^{i-2} (L_E L_\pi)^j d_E$. Letting $s'_i = \mu_E(s'_{i-1}, \mu_\pi(s'_{i-1}) + e_{i-1}^\pi) + \varepsilon_i^E$, we have the desired result.

We use this result to bound the difference in reward between the abstract and concrete rollouts when Algorithm 2 does not return a lower bound. For each i , because $s'_i \in \beta(s_{\text{original}_i}^\#)$ and $\mu_\pi(s'_i) + e_i^\pi \in \beta(a_i^\#)$, we define $r'_i = r(s'_i, \mu_\pi(s'_i) + e_i^\pi)$ and we know that $r' \in r_i^\#$. Because $\|s_i - s'_i\| \leq d_E \left(\frac{1 - (L_E L_\pi)^{i-1}}{1 - L_E L_\pi} \right)$ we have $\|a_i - a'_i\| \leq L_\pi d_E \left(\frac{1 - (L_E L_\pi)^{i-1}}{1 - L_E L_\pi} \right)$ and $|r(s_i, a_i) - r'_i| \leq L_r(1 + L_\pi)d_E \left(\frac{1 - (L_E L_\pi)^{i-1}}{1 - L_E L_\pi} \right)$. In particular, let $R' = \sum_i r'_i$ and then

$$|R(\tau) - R'| \leq \sum_{i=1}^T L_r(1 + L_\pi)d_E \left(\frac{1 - (L_E L_\pi)^{i-1}}{1 - L_E L_\pi} \right) = L_r(1 + L_\pi)d_E \frac{(L_E L_\pi)^T + (1 - L_E L_\pi)T - 1}{(1 - L_E L_\pi)^2}.$$

We now combine these two cases to bound the expected difference between the reward returned by Algorithm 2, denoted $R^\#(\tau)$, and the reward of τ . Let $D = R^\#(\tau) - R(\tau)$ be a random variable representing this difference. Then with

probability at least $(1 - \delta_E)^T$, $D \leq 0$ and in all other cases (i.e., with probability no greater than $1 - (1 - \delta_E)^T$), $D \leq L_R(1 + L_\pi)d_E \frac{(L_E L_\pi)^T + (1 - L_E L_\pi)T - 1}{(1 - L_E L_\pi)^2}$. In particular then,

$$\mathbb{E}[D] \leq \left(1 - (1 - \delta_E)^T\right) L_R(1 + L_\pi)d_E \frac{(L_E L_\pi)^T + (1 - L_E L_\pi)T - 1}{(1 - L_E L_\pi)^2}.$$

By definition $\mathbb{E}[R^\#(\tau)] = \mathbb{E}[R(\tau)] + \mathbb{E}[D]$. Therefore, we have

$$\mathbb{E}[R(\tau)] = \mathbb{E}[R^\#(\tau)] - \mathbb{E}[D] \geq \mathbb{E}[R^\#(\tau)] - \left(1 - (1 - \delta_E)^T\right) L_R(1 + L_\pi)d_E \frac{(L_E L_\pi)^T + (1 - L_E L_\pi)T - 1}{(1 - L_E L_\pi)^2}. \quad (3)$$

Algorithm 3 approximates $\mathbb{E}[R^\#(\tau)]$ by sampling N values. Let $\hat{R}^\#(\tau)$ be the measured mean and recall $\mathbb{E}[\hat{R}^\#(\tau)] = \mathbb{E}[R^\#(\tau)]$ and $\text{Var}[\hat{R}^\#(\tau)] = \text{Var}[R^\#(\tau)]/N$. Then by Chebyshev's inequality we have for all $k > 0$, $\Pr\left[\left|\hat{R}^\#(\tau) - \mathbb{E}[R^\#(\tau)]\right| \geq k\sqrt{\text{Var}[\hat{R}^\#(\tau)]}\right] \leq 1/k^2$. Then in particular, with probability at least $1 - 1/k^2$,

$$\hat{R}^\#(\tau) - k\sqrt{\frac{\text{Var}[R^\#(\tau)]}{N}} \leq R^\#(\tau).$$

Combining this with Equation 3 above and letting $k = 1/\sqrt{\delta}$, we have with probability at least $1 - \delta$,

$$\mathbb{E}[R(\tau)] \geq \hat{R}^\#(\tau) - \frac{1}{\sqrt{\delta}}\sqrt{\frac{\text{Var}[R^\#(\tau)]}{N}} - \left(1 - (1 - \delta_E)^T\right) L_R(1 + L_\pi)d_E \frac{(L_E L_\pi)^T + (1 - L_E L_\pi)T - 1}{(1 - L_E L_\pi)^2}.$$

□

C. Implementation Details

C.1. Training Details

We run our experiments on Quadro RTX 8000 and Nvidia T4 GPUs. We define the perturbation set $B(s)$ to be an l_∞ norm perturbation of the state with radius ϵ : $B_p(s, \epsilon) := \{s' \mid \|s' - s\| \leq \epsilon\}$ in the experiments. We use a smoothed linear ϵ -schedule during training as in (Zhang et al., 2020; Oikarinen et al., 2021). For the environments, we use the MuJoCo environments in OpenAI Gym (Brockman et al., 2016). We use Hopper-v2, HalfCheetah-v2, Ant-v2, Walker2d-v2 with 1000 trial length.

Network Structures and Hyperparameters for Training For both policy networks and the model networks, we use the same network as in (Pineda et al., 2021). For both MBPO and CAROL, we use the optimal hyperparameters in (Pineda et al., 2021). We mainly set two additional parameters, regularization parameters and the ϵ -schedule (Zhang et al., 2020; Oikarinen et al., 2021; Goyal et al., 2018) parameters for CAROL. The additional regularization parameter λ for regularizing L^{symbolic} is chosen in $\{0.1, 0.5, 1.0\}$. The ϵ -schedule starts as an exponential growth from $\epsilon = 10^{-12}$ and transitions smoothly into a linear schedule until reaching ϵ_{train} . Then the schedule keeps $\epsilon_t = \epsilon_{\text{train}}$ for the rest iterations. We set the temperature parameter controlling the exponential growth with 4.0 for all experiments. We have two other parameters to control the ϵ -schedule: *endStep*, and *finalStep*, where *endStep* is the step where ϵ_t reaches ϵ_{train} and *finalStep* is the steps for the total training. The *midStep* = $0.25 * \text{endStep}$ is the turning point from the exponential growth to the linear growth. Table 3 shows the details of each parameters.

C.2. Certificate Usage

In evaluation, we compare the certified performance of policies trained from different algorithms with a set of environment models. We train these models based on the rollout trajectory dataset for 4×10^5 environment steps between 5 policies and the environment. Among these 5 policies, three of them are trained from MBPO and the remaining are trained from SAC (Haarnoja et al., 2018), which is the base algorithm without model for MBPO.

Environments	Methods	<i>endStep</i>	<i>finalStep</i>
Hopper	CAROL	4×10^5	5×10^5
	CAROL-SS	4×10^5	5×10^5
Ant	CAROL	8×10^5	9×10^5
	CAROL-SS	4×10^6	5×10^6
Walker2d	CAROL	7×10^5	7.5×10^5
	CAROL-SS	1.5×10^6	2×10^6
HalfCheetah	CAROL	7.5×10^5	8.5×10^5
	CAROL-SS	7.5×10^5	8.5×10^5

Table 3: Parameters for ϵ -schedule.